25

Robust Bilateral Control for Teleoperation System with Communication Time Delay - Application to DSD Robotic Forceps for Minimally Invasive Surgery -

Chiharu Ishii
Hosei University
Japan

1. Introduction

Minimally invasive surgery (MIS) has excellent characteristics that can reduce the burden on patients. However, surgeons experience great difficulties in operation due to limitations in dexterity imposed by the surgical instruments and the small work space. Therefore, the development of surgical assistance devices with the application of robotic and mechatronic technology is in high demand (Taylor & Stoianovici, 2003).

Recently, robotic surgical support systems such as `da VINCI' are in clinical use (Guthart & Salisbury, 2000). In particular, the development of multi-DOF robotic forceps manipulators capable of reproducing complex human finger movements in laparoscopic surgery is one of the most important issues in the field of robotic surgical systems.

A large number of conventional multi-DOF robotic forceps manipulators currently available for MIS are of the wire actuation type (Ikuta et al., 2003). However, the rigidity and the durability of wires are poor. Furthermore, cleaning and sterilization of the wire are problematic.

In order to improve the rigidity and the sterilization capability of the manipulator, multi-DOF robotic forceps manipulators which use methods different from wire actuation for bending motion have been developed. These are roughly divided into two types. The first type is where two-DOF bending is achieved by combining independent joints which perform yaw and pitch motions, respectively. The second type is where omnidirectional two-DOF bending is achieved by inclination of the entire bending part of the forceps. Many manipulators of the first type are linkage-driven forceps manipulators. In (Yamashita et al., 2005), an endoscopic forceps manipulator using a multi-slider linkage mechanism is developed without using wires for bending motion. However, a wire is used for gripping motion. In (Arata et al., 2005), a linkage-driven forceps manipulator which does not use wires for either bending or gripping motions is developed.

On the other hand, as one of the omnidirectional driven-type forceps manipulators, an active forceps manipulator in the form of a tripodal platform is developed in (Kobayashi et al., 2002). Although it has high rigidity, its bending range is 40 to 50 degrees, and it is difficult to expand the bending range due to constraints inherent in the mechanism.

We have developed a multi-DOF robotic forceps manipulator for minimally invasive surgery incorporating a novel omnidirectional bending technique with a screw drive mechanism, termed Double-Screw-Drive (DSD) mechanism, so far (Ishii et al., 2010). A robotic forceps manipulator incorporating the DSD mechanism (DSD robotic forceps) can bend without using wires. Without wires, it has high rigidity, and it can bend at 90 degrees in any arbitrary direction. In addition, the gripper of the DSD robotic forceps can perform rotational motion. Opening and closing motions of the gripper are attained by wire actuation.

In order to improve the operability of the robotic surgical support systems and to help surgeon's dexterity, development of haptic forceps teleoperation systems is required. Most recently, haptic forceps manipulator for minimally invasive surgery has been proposed in (Seibold et al., 2005) and (Zemiti et al., 2007), in which operation force is measured by sensor and force feedback is provided. In addition, the motion scaling, which can adequately reduce or enlarge the movements and tactile senses of the operator and the robot, is necessary to assure safety of the surgery.

On the other hand, communication time delay is inevitable in teleoperation systems, which may causes instability of the teleoperation systems. Therefore, stability of the system must be guaranteed in the presence of the communication time delay between master device and slave device. For bilateral teleoperation systems with constant time delay, stabilization method based on scattering transformation is proposed in (Anderson & Spong, 1989). (Chopra & Spong, 2005) proposed a passivity based control scheme which guarantees delay dependent exponential stability of the position and velocity tracking error. However, coupling torques are given as a function of position and velocity, and is not a function of force. Hence, motion scaling in force tracking cannot be achieved.

In this chapter, improving the control scheme proposed in (Chopra & Spong, 2005), such a passivity based bilateral control scheme that enables motion scaling in both position tracking and force tracking, and guarantees the stability of the teleoperation system in the presence of constant time delay, is proposed. This can be achieved by adding force tracking error terms to the coupling torques.

Then, the proposed bilateral control scheme is applied to a haptic control of bending motion of the DSD robotic forceps teleoperation system with constant time delay. However, the proposed bilateral control law is applicable only to the one-DOF bending motion of the DSD robotic forceps. Therefore, using the change of coordinates, the proposed bilateral control scheme is extended so that it may become applicable to the omnidirectional bending motion of the DSD robotic forceps.

Experimental works were carried out using the proposed bilateral control scheme, and experimental results showed the effectiveness of the proposed control scheme.

2. DSD robotic forceps

In this section, details of the DSD robotic forceps are explained. Overview of the developed DSD robotic forceps manipulator is shown in Fig. 1, and the configuration of its bending part is shown in Fig. 2.

2.1 Specifications

The total length of the DSD robotic forceps manipulator is 635 mm, and its gross weight is 1050 g. The main specifications of the DSD robotic forceps are given as follows.

1. In order to insert a forceps into a trocar, the diameter of the rod of the forceps must be 10 mm or less since the diameter of the trocar is 12 mm.
2. The bending force, defined as the lifting force at the tip of the forceps, must be larger than 4 N, which would allow the forceps to lift 1/3 of an average human liver. This ability is required during operations of internal organs under the liver.
3. The bending range must be 180 (-90 to +90) degrees or more in both horizontal and vertical direction. This ability is required in order to obtain a sufficient degree of freedom in limited work space.
4. The gripper must be able to perform opening and closing motions smoothly. This operational requirement is necessary for the proper holding and releasing of medical needles.
5. In order to perform suturing in a small work space, such as the opposite or the far side of internal organs, the gripper of the forceps must be able to rotate.

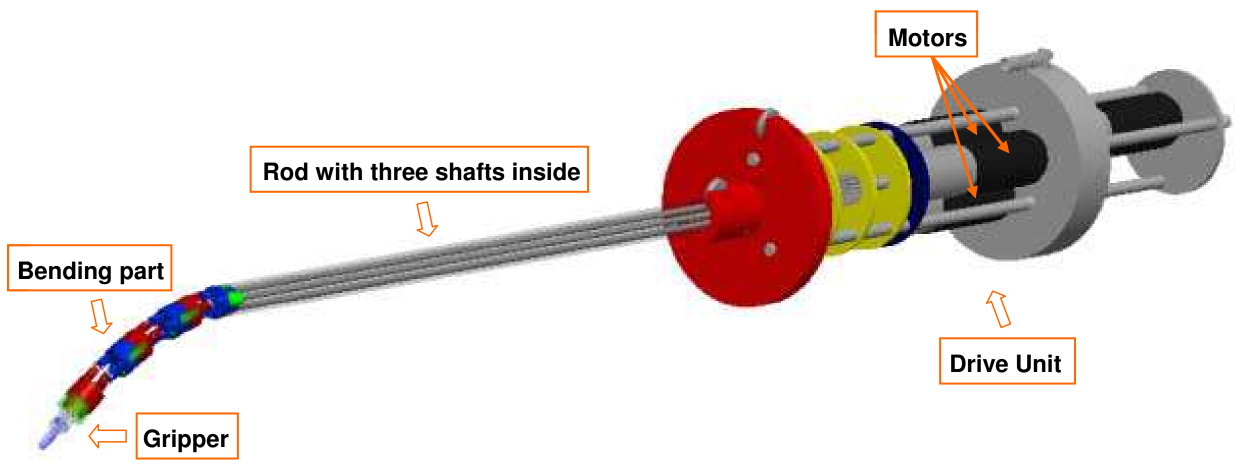

Fig. 1. Overview of DSD robotic forceps manipulator

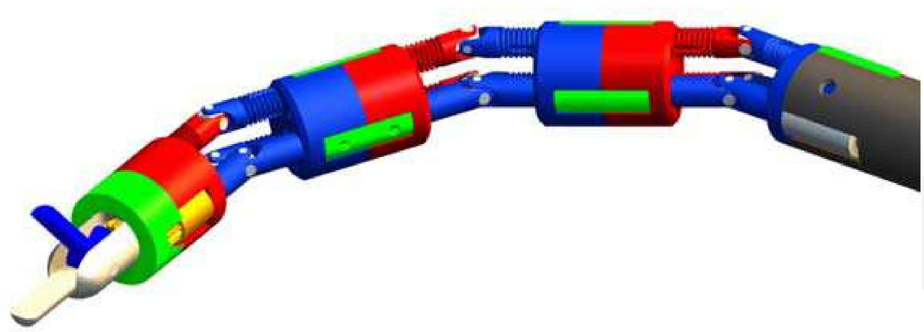

Fig. 2. Bending part of DSD robotic forceps manipulator

2.2 Bending mechanism

One module of the bending mechanism is shown in Fig.3.

The DSD mechanism has three linkages, and when examined in cross-sectional view, each linkage is 120 degrees apart from the other linkages and 6 mm from the center of the cross-section. Let us denote the group consisting of part ⑤ and part ⑥ as a “bending linkage” and the group consisting of part ① and part ② as a “grasping linkage”. Bending motion is achieved by rotating the two bending linkages, and grasping linkage is used for actuating the gripper. The key point of this mechanism is that one side of part ⑤ is a left-handed screw and the other side is a right-handed screw. When a DSD module is connected to another module, a joint is formed. The principle of the bending motion for such a joint is illustrated in Fig. 4.

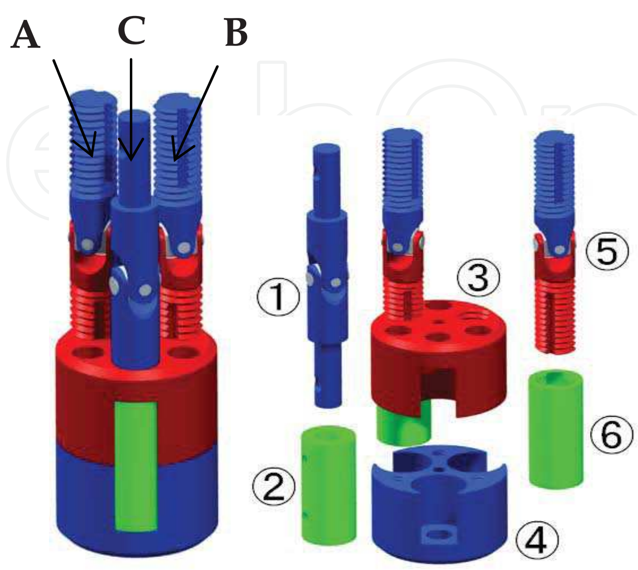

A and B: Bending linkage, C: Grasping linkage

① Universal joint shaft
② Coupling
③ Plate with left-handed threaded hole
④ Plate with right-handed threaded hole
⑤ Universal joint of the screw drive
⑥ Spline nut

Fig. 3. One module of DSD mechanism

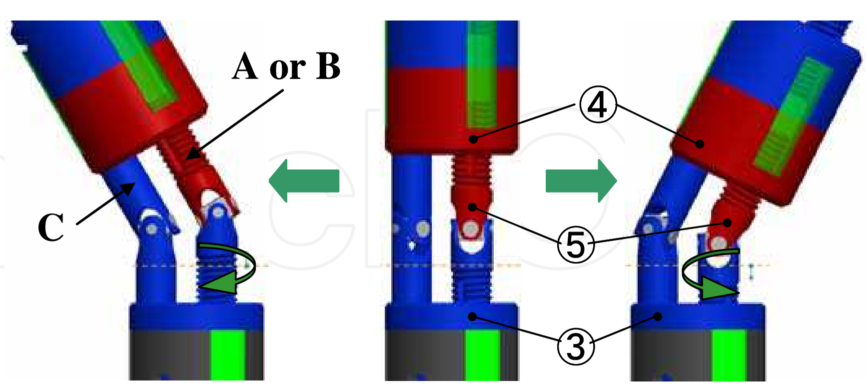

Fig. 4. Principle of bending motion

The left-handed screw of part ⑤ connects to part ③, and the right-handed screw of part ⑤ connects to part ④ of another module. The rotation of the linkage changes the connecting length of the screw and the plate at both ends of part ⑤. As a result, an angle is formed between part ③ and part ④. For example, when the linkage rotates clockwise, part ③ and part ④ approach each other, and when the linkage rotates counterclockwise, they move away from each other. Thus, bending motion is achieved. The maximum bending angle of one joint is between -30 and +30 degrees since this is the allowable bending angle of the universal joint. One bending linkage allows for one-DOF bending motion, and by using two bending linkages and controlling their rotation angles, arbitrary omnidirectional bending motion can be attained. The total length of the bending part is 59 mm excluding a gripper.

2.3 Attachment and rotary gripper

The gripper is exchangeable as an end effector and can be replaced with tools such as scalpels or surgical knives. Fig. 5 shows the attachment of the end effecter and mechanism of the rotary gripper. Gear 1 is on the tip of the grasping linkage and gear 2 is at the root of the jaw mesh. The gripper is turned by rotation of the grasping linkage. Although the rotary gripper can rotate arbitrary degrees, it should be rotated within 360 degrees to avoid winding of the wire which drives the jaw.

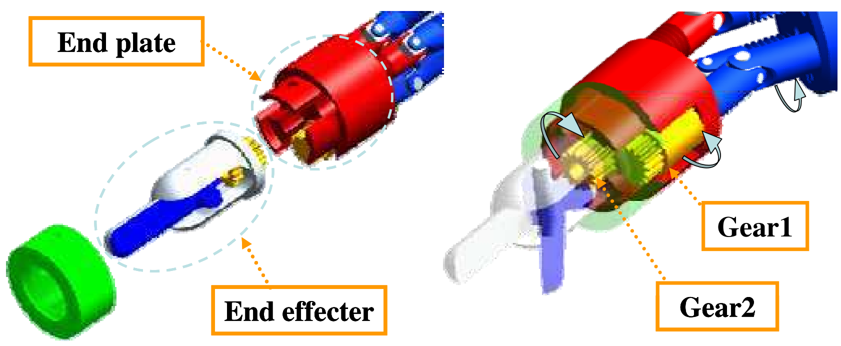

Fig. 5. Attachment and rotation of gripper

2.4 Open and close of jaws

The opening and closing motions of the gripper are achieved by wire actuation. Only one side of the jaws can move, and the other side is fixed. The wire for actuation connects to the drive unit through the inside of the DSD mechanism and the rod, and is pulled by the motor. The open and closed states of the gripper are shown in Fig.6.

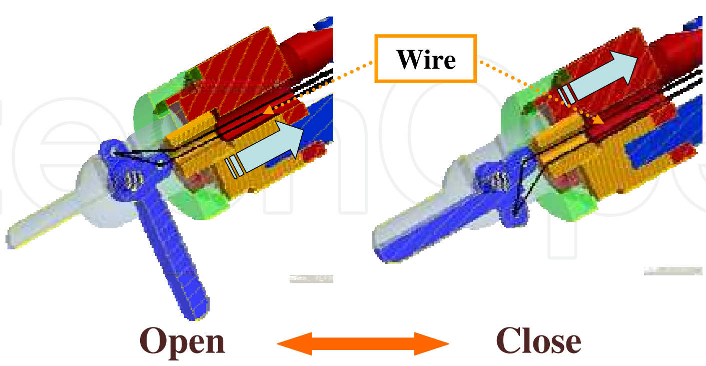

Fig. 6. Grasping of gripper

2.5 Drive unit

The feature of a drive unit for the DSD robotic forceps manipulator is shown in Fig.7. The total length of the drive unit is 274 mm, its maximum diameter is 50 mm, and its weight is 935 g. Driving forces from motors are transmitted to the linkages through the gears. There are four motors in the drive unit. Three motors are mounted at the center of the drive unit. Two of them are used for inducing bending motion and the third one is used for inducing rotary motion of the gripper. The fourth motor, which is mounted in the tail, is for the opening and closing motions of the gripper actuated by wire. The wire capstan is attached to the motor shaft of the forth motor and acts as a reel for the wire. The spring is used for maintaining the tension of the wire. DC micromotors 1727U024C (2.25W) produced by FAULHABER Co. were selected for the bending motion and the rotary motion of the gripper. For the opening and closing motions of the gripper, a DC micro motor 1727U012C (2.25W) produced by FAULHABER Corp. was selected. A reduction gear and a rotary encoder are installed in the motor.

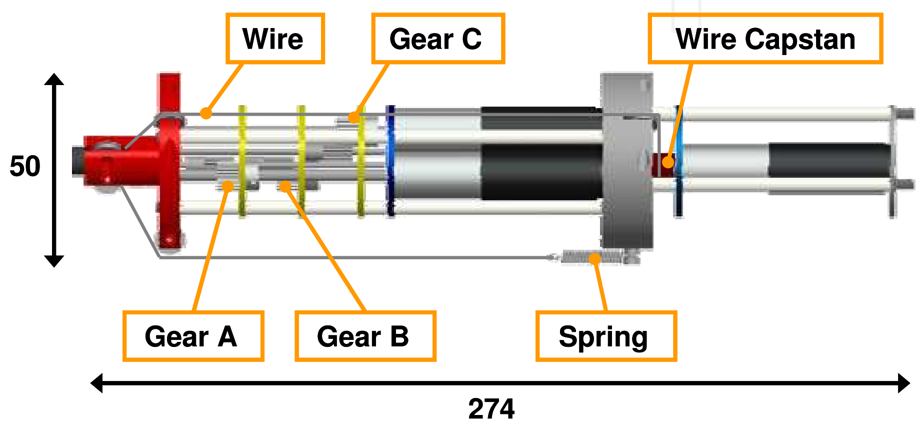

Fig. 7. Drive unit

The inside part of the rod, as shown in Fig. 1, consists of three shafts, each 2 mm in diameter and 300 mm long. Each motor in the drive unit and each linkage in the DSD mechanism are connected to each other through a shaft. Therefore, the rotation of each motor is transmitted to each respective linkage through a shaft.

2.6 Built DSD robotic forceps manipulator

The proposed DSD robotic forceps manipulator was built from stainless steel SUS303 and SUS304 to satisfy bio-compatibility requirements. The miniature universal joints produced by Miyoshi Co., LTD. were selected. The universal joints have a diameter of 3 mm and are of the MDDS type. The screws on both sides of the yokes were fabricated by special order.
The built DSD robotic forceps manipulator is shown in Fig. 8. Its maximum diameter from the top of the bending part to the root of the rod is 10 mm. The total length of the bending part, including the gripper, is 85 mm.

Fig. 8. Built DSD robotic forceps manipulator

A transition chart of the rotary gripper is shown in Fig.9.

Fig. 9. Transition chart of the rotary gripper

2.7 Master manipulator for teleoperation

In a laparoscopic surgery, multi-DOF robotic forceps manipulators are operated by remote control. In order to control the DSD robotic forceps as a teleoperation system, the joy-stick type master manipulator for teleoperation was designed and built in (Ishii et al., 2010) by reconstruction of a ready-made joy-stick combined with the conventional forceps, which enables to control bending, grasping and rotary motions of the DSD robotic forceps manipulator. In addition, the built joy-stick type master manipulator was modified so that the operator can feel reaction force generated by the electric motors. The teleoperation system and the force feedback mechanisms for the bending force are illustrated in Fig.10. The operation force is detected by the strain gauges, and variation of the position is measured by the encoders mounted in the electric motors.

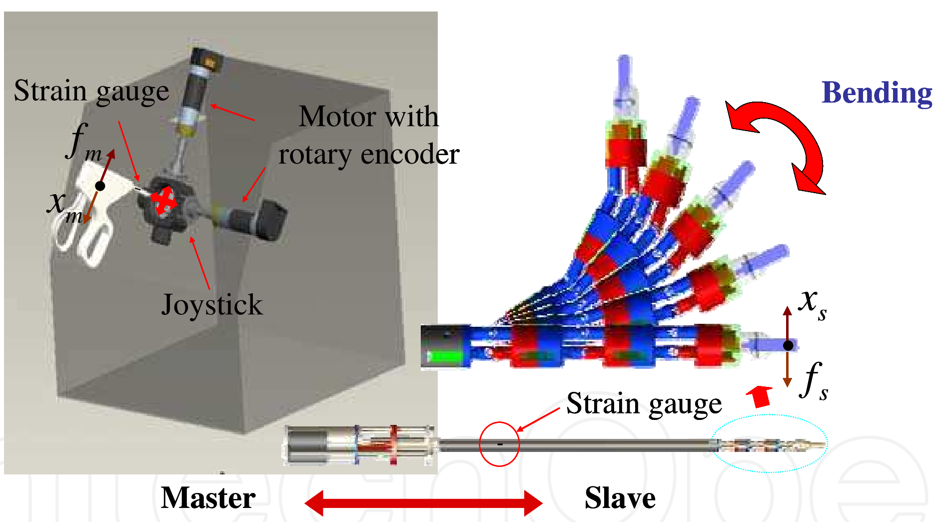

Fig. 10. DSD robotic forceps teleoperation system

3. Bilateral control for one-DOF bending

In this section, bilateral control law for one-DOF bending of the DSD robotic forceps teleoperation system with communication time delay is derived.

3.1 Derivation of Control Law

Let the dynamics of the one-DOF master-slave teleoperation system be given by

$$m_m\ddot{x}_m + b_m\dot{x}_m + c_m x_m = \tau_m + f_m , \tag{1}$$

$$m_s\ddot{x}_s + b_s\dot{x}_s + c_s x_s = \tau_s - f_s \,, \tag{2}$$

where subscripts m and s denote master and slave respectively. x_m and x_s represent the displacements, m_m and m_s the masses, b_m and b_s the viscous coefficients, and c_m and c_s the spring coefficients of the master and slave devices. f_m stands for the force applied to the master device by human operator, f_s the force of the slave device due to the mechanical interaction between slave device and handling object, and τ_m and τ_s are input motor toques.

As shown in Fig.11, there exists constant time delay T in the network between the master and the slave systems.

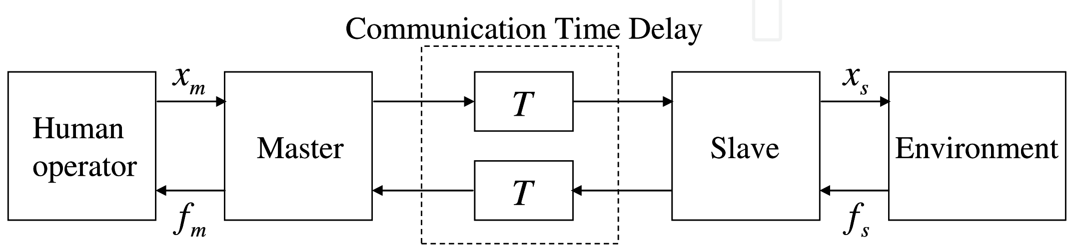

Fig. 11. Communication time delay in teleoperation systems

Define motor torques as

$$\tau_m = \bar{\tau}_m - m_m\lambda\dot{x}_m - b_m\lambda x_m + c_m x_m \,, \tag{3}$$

$$\tau_s = \bar{\tau}_s - m_s\lambda\dot{x}_s - b_s\lambda x_s + c_s x_s \,, \tag{4}$$

where λ is a positive constant, and $\bar{\tau}_m$ and $\bar{\tau}_s$ are coupling torques. Then, the dynamics are rewritten as follows.

$$m_m\dot{r}_m + b_m r_m = \bar{\tau}_m + f_m \,, \tag{5}$$

$$m_s\dot{r}_s + b_s r_s = \bar{\tau}_s - f_s \,, \tag{6}$$

where r_m and r_s are new variables defined as

$$r_m = \dot{x}_m + \lambda x_m \,, \tag{7}$$

$$r_s = \dot{x}_s + \lambda x_s \,. \tag{8}$$

Control objective is described as follows.

[Design Problem] Find a bilateral control law which satisfies the following two specifications.

Specification 1: In both position tracking and force tracking, the motion scaling, which can adequately reduce or enlarge the movements and tactile senses of the master device and the slave device, is achievable.

Specification 2: The stability of the teleoperation system in the presence of the constant communication time delay between master device and slave device, is guaranteed.

Assume the following condition.
Assumption: The human operator and the remote environment are passive.
In the presence of the communication time delay between master device and slave device, the following fact is shown in (Chopra et al., 2003).
Fact: In the case where the communication time delay T is constant, the teleoperation system is passive.
From Assumption and Fact, the following inequalities hold.

$$-\int_0^t r_m f_m d\tau \geq 0, \quad \int_0^t r_s f_s d\tau \geq 0, \tag{9}$$

$$-\int_0^t r_s f_m(\tau - T) d\tau \geq 0, \quad \int_0^t r_m f_s(\tau - T) d\tau \geq 0. \tag{10}$$

Using inequalities (9) and (10), define a positive definite function V as follows.

$$\begin{aligned} V = & m_m r_m{}^2 + G_p m_s r_s{}^2 + K_1 \int_{t-T}^t \left(r_m{}^2 + G_p{}^2 r_s{}^2 \right) d\tau \\ & -2(K_m + 1)\int_0^t r_m f_m d\tau + 2G_p \left(G_f K_s + 1 \right) \int_0^t r_s f_s d\tau \\ & -2G_p K_s \int_0^t r_s f_m(\tau - T) d\tau + 2G_f K_m \int_0^t r_m f_s(\tau - T) d\tau \end{aligned}, \tag{11}$$

where K_1, K_m and K_s are feedback gains, and $G_p \geq 1$ and $G_f \geq 1$ are scaling gains for position tracking and force tracking, respectively.
The derivative of V along the trajectories of the systems (5) and (6) is given by

$$\begin{aligned} \dot{V} = & 2m_m r_m \dot{r}_m + 2G_p m_s r_s \dot{r}_s + K_1 \left(r_m{}^2 + G_p{}^2 r_s{}^2 \right) \\ & - K_1 \left(r_m{}^2(t-T) + G_p{}^2 r_s{}^2(t-T) \right) \\ & - 2(K_m + 1) r_m f_m + 2G_p \left(G_f K_s + 1 \right) r_s f_s \\ & - 2G_p K_s r_s f_m(t-T) + 2G_f K_m r_m f_s(t-T) \\ = & 2r_m\left(-b_m r_m + \overline{\tau}_m + f_m \right) + 2G_p r_s \left(-b_s r_s + \overline{\tau}_s - f_s \right) \\ & - K_1 \left(G_p r_s(t-T) - r_m \right)\left(G_p r_s(t-T) + r_m \right) \\ & - K_1 \left(r_m(t-T) - G_p r_s \right)\left(r_m(t-T) + G_p r_s \right) \\ & - 2(K_m + 1) r_m f_m + 2G_p \left(G_f K_s + 1 \right) r_s f_s \\ & - 2G_p K_s r_s f_m(t-T) + 2G_f K_m r_m f_s(t-T). \end{aligned} \tag{12}$$

Let the coupling torques be given as follows.

$$\overline{\tau}_m = K_1 \left(G_p r_s(t-T) - r_m \right) - K_m \left(G_f f_s(t-T) - f_m \right), \tag{13}$$

$$\overline{\tau}_s = K_1 \left(r_m(t-T) - G_p r_s \right) + K_s \left(f_m(t-T) - G_f f_s \right). \tag{14}$$

Using (13) and (14), (12) is rewritten as follows.

$$
\begin{aligned}
\dot{V} &= -2b_m r_m{}^2 + 2r_m\bar{\tau}_m + 2r_m f_m - 2G_p b_s r_s{}^2 + 2G_p r_s\bar{\tau}_s - 2G_p r_s f_s \\
&\quad + \left\{\bar{\tau}_m + K_m\left(G_f f_s(t-T) - f_m\right)\right\}\left[2r_m + K_1{}^{-1}\left\{\bar{\tau}_m + K_m\left(G_f f_s(t-T) - f_m\right)\right\}\right] \\
&\quad - \left\{\bar{\tau}_s - K_s\left(f_m(t-T) - G_f f_s\right)\right\}\left[2G_p r_s + K_1{}^{-1}\left\{\bar{\tau}_s - K_s\left(f_m(t-T) - G_f f_s\right)\right\}\right] \\
&\quad - 2\left(K_m+1\right)r_m f_m + 2G_p\left(G_f K_s + 1\right)r_s f \\
&\quad - 2G_p K_s r_s f_m(t-T) + 2G_f K_m r_m f_s(t-T) \\
&= -2b_m r_m{}^2 - 2G_p b_s r_s{}^2 \\
&\quad - K_1{}^{-1}\left\{\bar{\tau}_m + K_m\left(G_f f_s(t-T) - f_m\right)\right\}^2 - K_1{}^{-1}\left\{\bar{\tau}_s - K_s\left(f_m(t-T) - G_f f_s\right)\right\}^2 \\
&\le -K_1\left(G_p r_s(t-T) - r_m\right)^2 - K_1\left(r_m(t-T) - G_p r_s\right)^2 .
\end{aligned}
\tag{15}
$$

Thus, stability of the teleoperation system is assured in spite of the presence of the constant communication time delay, and delay independent exponential convergence of the tracking errors of position to the origin is guaranteed.
Finally, motor torques (3) and (4) are given as follows.

$$
\begin{aligned}
\tau_m &= K_1 G_p \dot{x}_s(t-T) + \lambda K_1 G_p x_s(t-T) - K_m G_f f_s(t-T) \\
&\quad -\left(K_1 + \lambda m_m\right)\dot{x}_m + \left(c_m - \lambda(K_1 + b_m)\right)x_m + K_m f_m
\end{aligned} ,
\tag{16}
$$

$$
\begin{aligned}
\tau_s &= K_1 \dot{x}_m(t-T) + \lambda K_1 x_m(t-T) + K_s f_m(t-T) \\
&\quad -\left(K_1 G_p + \lambda m_s\right)\dot{x}_s + \left(c_s - \lambda(K_1 G_p + b_s)\right)x_s - K_s f_s
\end{aligned} .
\tag{17}
$$

3.2 Experiments

In order to verify an effectiveness of the proposed control law, experimental works were carried out for the developed DSD robotic forceps teleoperation system. Here, only vertical direction of the bending motion is considered. Namely, bending motion of the DSD robotic forceps is restricted to one degree of freedom. Then, the dynamics of the master-slave teleoperation system are given by equations (1) and (2), since only one bending linkage is used. Parameter values of the system are given as m_m = 0.07 kg, m_s = 0.025 kg, b_m = 0.25 Nm/s, b_s = 2.5 Nm/s, c_m = 9 N/s and c_s = 9 N/s. The control system is constructed under the MATLAB/Simulink software environment.
In the experiments, 200g weights pet bottle filled with water was hung up on the tip of the forceps, and lift and down were repeated in vertical direction. Appearance of the experiment is shown in Fig. 12.
First, in order to see the effect of the motion scaling, experimental works with the following conditions were carried out.

a. Verification of the effect of the motion scaling.
   i) G_p= G_f = 1 and T = 0
   ii) G_p = 2, G_f = 3 and T = 0

Second, in order to see the effect to the time delay, comparison of the proposed bilateral control scheme and conventional bilateral control method was performed.

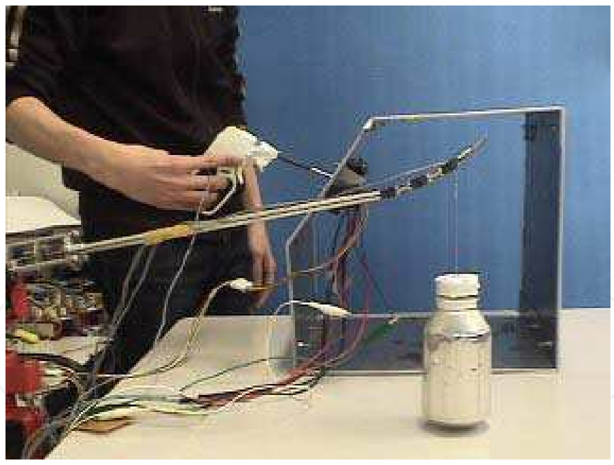

Fig. 12. Appearance of experiment

b. Verification of the effect to the time delay.
i) $G_p = G_f = 1$ and $T = 0.125$
ii) Force reflecting servo type bilateral control law with constant time delay $T = 0.125$

In b-ii), the force reflecting servo type bilateral control law is given as follows.

$$\tau_m = K_f\left(f_m - f_s(t-T)\right), \tag{18}$$

$$\tau_s = K_p\left(x_m(t-T) - x_s\right), \tag{19}$$

where K_f and K_p are feedback gains of force and position. The time delay T = 0.125 is intentionally generated in the control system, whose value was referred from (Arata et al., 2007) as the time delay of the control signal between Japan and Thailand: approximately 124.7 ms.

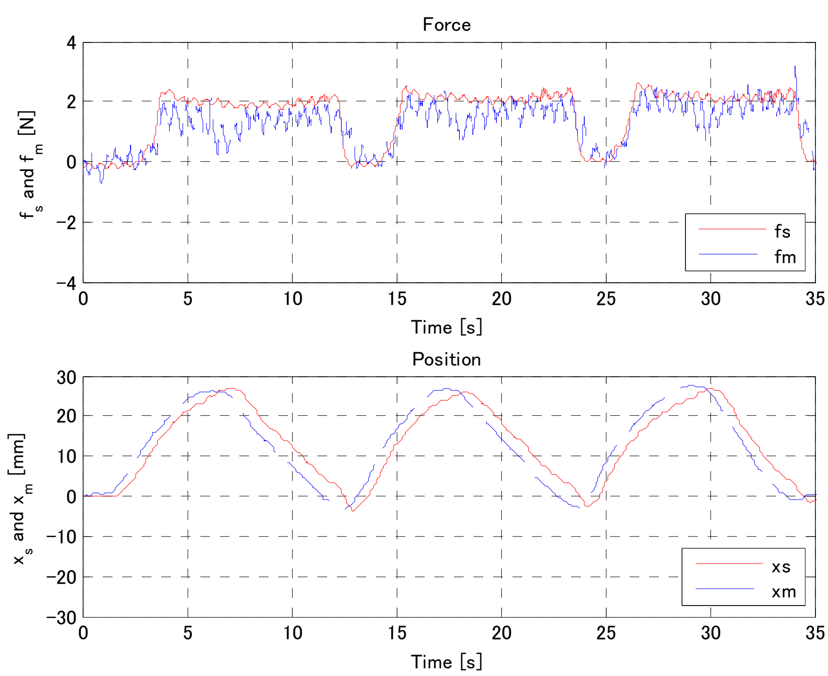

Fig. 13. Experimental result for a-i)

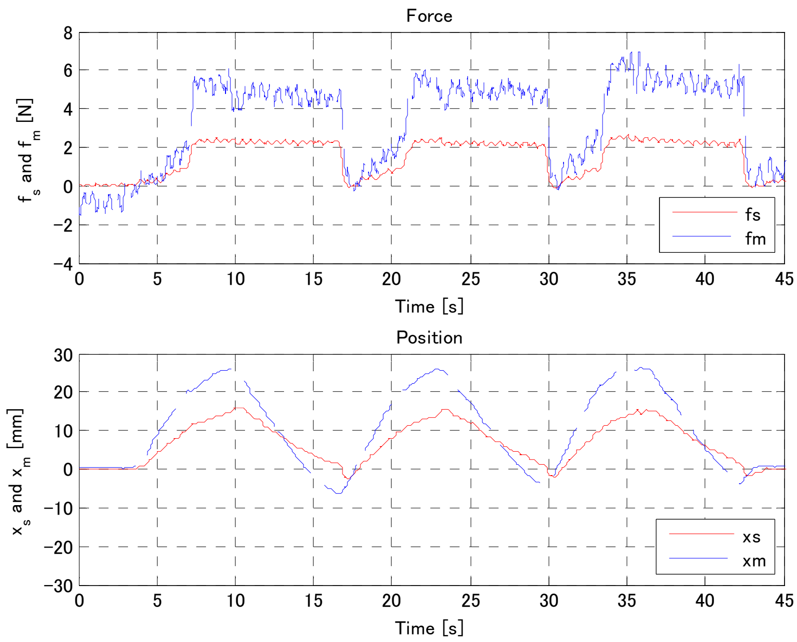

Fig. 14. Experimental result for a-ii)

Note that the proposed bilateral control scheme guarantees stability of the teleoperation system in the presence of constant time delay, however, stability is not guaranteed in use of the force reflecting servo type bilateral control law in the presence of constant time delay.

Feedback gains were adjusted by trial and error through repetition of experiments, which were determined as λ = 3.8, K_1 = 30, K_m = 400, K_s = 400, K_p = 60 and K_f = 650. Experimental results for condition a) are shown in Fig. 13 and Fig. 14.

As shown in Fig. 13 and Fig. 14, it is verified that the motion of slave tracks the motion of master with specified scale in both position tracking and force tracking.

Experimental results for condition b) are shown in Fig. 15 and Fig. 16.

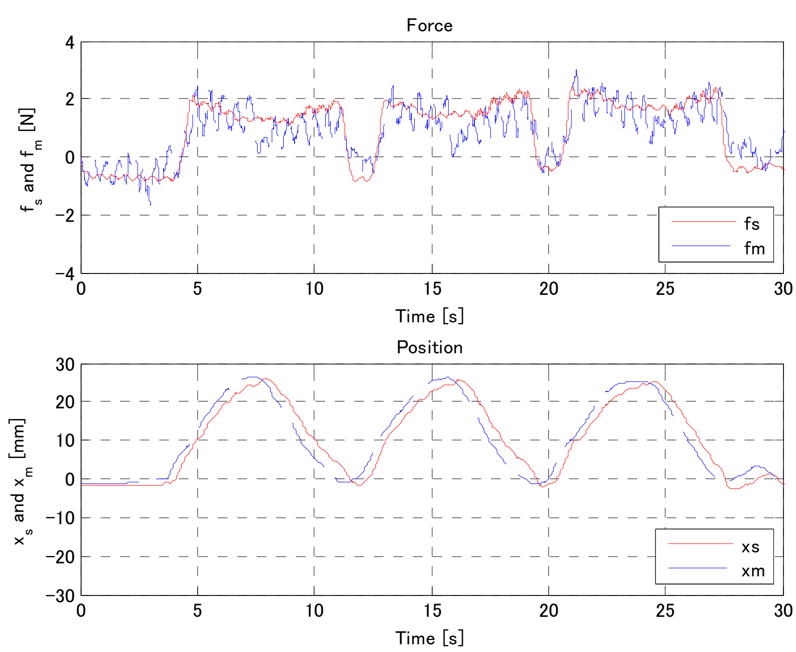

Fig. 15. Experimental result for b-i)

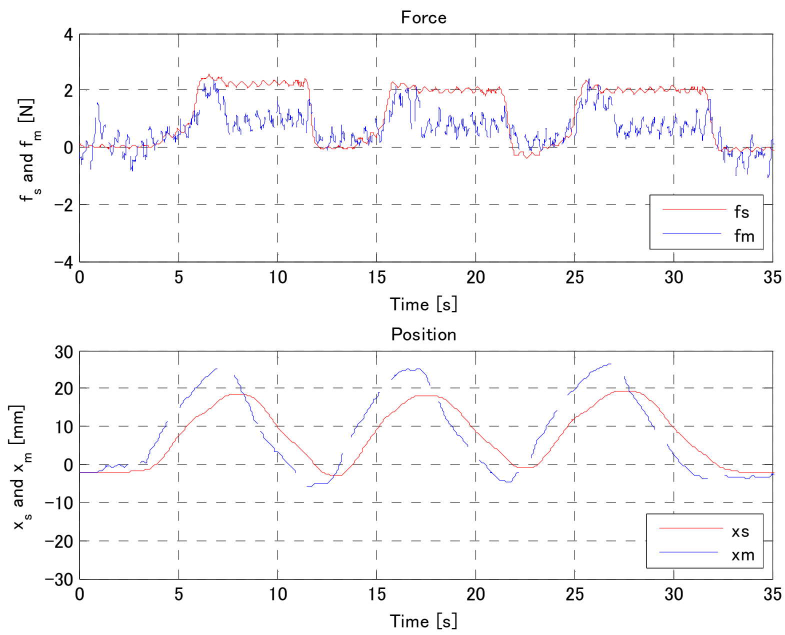

Fig. 16. Experimental result for b-ii)

As shown in Fig. 15 and Fig. 16, tracking errors of both position and force in Fig. 15 are smaller than those of Fig. 16. From the above observations, the effectiveness of the proposed control law for one-DOF bending motion of the DSD robotic forceps was verified.

4. Bilateral control for omnidirectional bending

In this section, the bilateral control scheme described in the former session is extended to omnidirectional bending of the DSD robotic forceps teleoperation system with constant time delay.

4.1 Extension to omnidirectional bending

As shown in Fig.10, master device is modified joy-stick type manipulator. Namely, this is different structured master-slave system. The cross-section views of shaft of the joy-stick and the DSD robotic forceps are shown in Fig.17.

Due to the placement of strain gauges and motors with encoder of the master device, the dynamics of the master device are given in *x*-*y* coordinates as follows.

$$m_m \ddot{x}_m + b_m \dot{x}_m + c_m x_m = \tau_{xm} + f_{xm}, \tag{20}$$

$$m_m \ddot{y}_m + b_m \dot{y}_m + c_m y_m = \tau_{ym} + f_{ym}. \tag{21}$$

When only motor *A* drives, bending direction of the DSD robotic forceps is along *A*-axis, and when only motor *B* drives, bending direction of the DSD robotic forceps is along *B*-axis. Thus, due to the arrangement of the bending linkages, the dynamics of the slave device are given in *A*-*B* coordinates as follows.

$$m_s \ddot{A}_s + b_s \dot{A}_s + c_s A_s = \tau_{As} - f_{As}, \tag{22}$$

$$m_s \ddot{B}_s + b_s \dot{B}_s + c_s B_s = \tau_{Bs} - f_{Bs}. \tag{23}$$

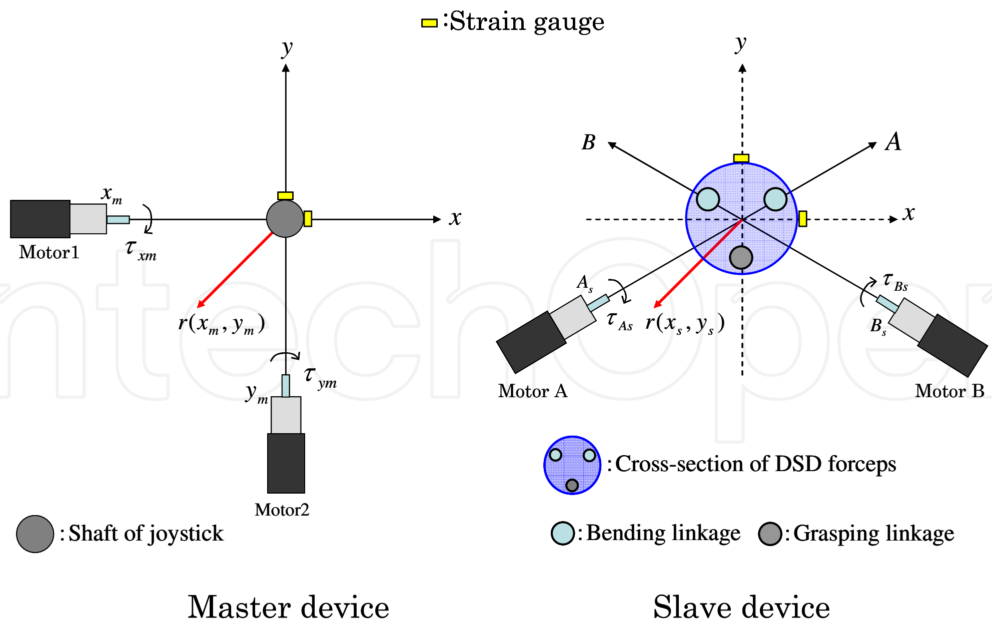

Fig. 17. Coordinates of master device and slave device

In order to extend the proposed bilateral control law to the omnidirectional bending motion of the DSD robotic forceps, the coordinates must be unified.

As shown in Fig. 17, x_m and y_m are measured by encoders. f_{xm}, f_{ym}, f_{xs}, and f_{ys} are measured by strain gauges. τ_{xm}, τ_{ym}, τ_{xs} and τ_{ys} are calculated from the bilateral control laws. These values are obtained in x-y coordinates. Therefore, consider to unify the coordinates in x-y coordinates. While, displacement of the slave A_s and B_s are measured by encoder, which are obtained in A-B coordinates. These values must be changed into x-y coordinates.

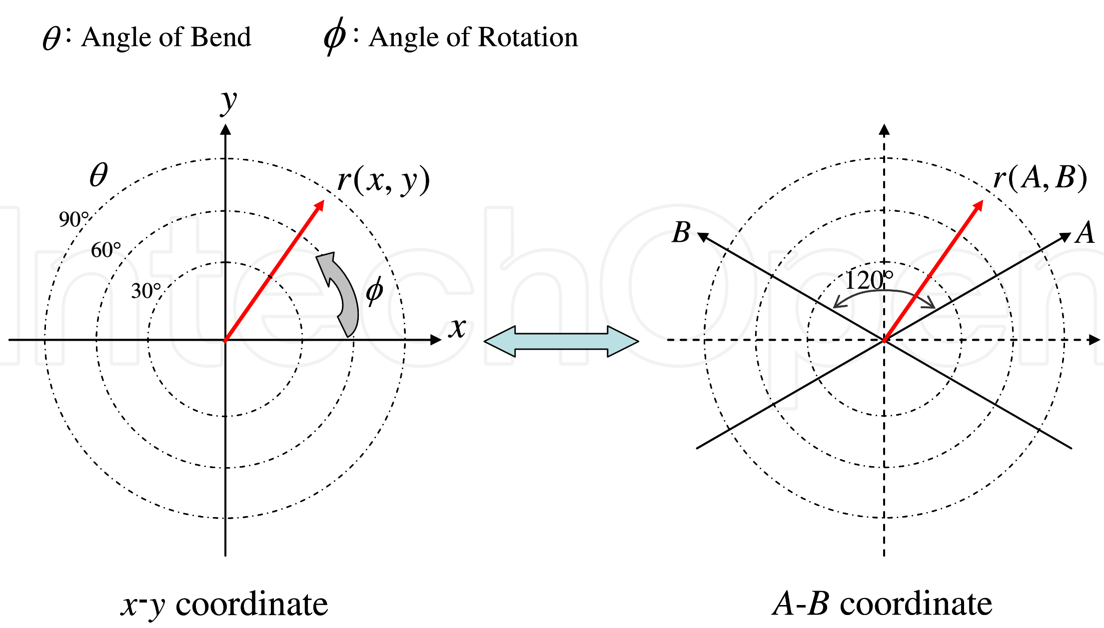

Fig. 18. Change of coordinates

The change of coordinates for position $r(A,B)$ given in A-B coordinates to $r(x,y)$ given in x-y coordinates (Fig. 18) is given as follows.

$$\begin{bmatrix} x \\ y \end{bmatrix} = \frac{1}{2}\begin{bmatrix} \sqrt{3} & -\sqrt{3} \\ 1 & 1 \end{bmatrix}\begin{bmatrix} A \\ B \end{bmatrix}. \tag{24}$$

Thus, the dynamics of the slave device given in *A*-*B* coordinates are converted into *x*-*y* coordinates. Finally, the dynamics of the two-DOF DSD robotic forceps teleoperation system in horizontal direction and vertical direction are described as follows.

$$\begin{cases} m_m\ddot{x}_m + b_m\dot{x}_m + c_m x_m = \tau_{xm} + f_{xm} \\ m_s\ddot{x}_s + b_s\dot{x}_s + c_s x_s = \tau_{xs} - f_{xs} \end{cases} \tag{25}$$

$$\begin{cases} m_m\ddot{y}_m + b_m\dot{y}_m + c_m y_m = \tau_{ym} + f_{ym} \\ m_s\ddot{y}_s + b_s\dot{y}_s + c_s y_s = \tau_{ys} - f_{ys} \end{cases} \tag{26}$$

For each direction, the bilateral control law derived in the former session, which is developed for one-DOF bending of the DSD robotic forceps, is applied.
However, as shown in Fig. 17, the actual torque inputs to the motors in the slave device are τ_{As} and τ_{Bs}. Therefore, input torque of the slave must be given in *A*-*B* coordinates. τ_{As} and τ_{Bs} can be obtained from τ_{xs} and τ_{ys} through an inverse transformation of (24), which is given by

$$\begin{bmatrix} \tau_{As} \\ \tau_{Bs} \end{bmatrix} = \begin{bmatrix} 1/\sqrt{3} & 1 \\ -1/\sqrt{3} & 1 \end{bmatrix}\begin{bmatrix} \tau_{xs} \\ \tau_{ys} \end{bmatrix}. \tag{27}$$

Thus, bilateral control for the omnidirectional bending motion of the DSD robotic forceps is realized.

4.2 Experiments

Experimental works were carried out using the proposed bilateral control laws. The parameter values of the system are given as same value as described in subsection 3.2.
In the experiments, 100g weight pet bottle filled with water was hung up on the tip of the forceps, and the pet bottle was lifted by vertical bending motion of the forceps. Then, the forceps was controlled so that the tip of the forceps draws a quarter circular orbit counterclockwise, and the PET bottle was landed on the floor.
Experimental works were carried out under the communication time delay T = 0.125. The control gains were determined by trial and error through the repetition of experiments, which are given as λ = 5.0, K_1 = 40, K_m = 80, and K_s = 80. Scaling gains were chosen as G_p= G_f = 1. Experimental results are shown in Fig. 19.
In Fig. 19, the top two figures show force and position in *x* coordinates, and the bottom two figures show force and position in *y* coordinates. In the experiment, the PET bottle was lifted at around 4 seconds, and landed on the floor at around 20 seconds. The counterclockwise rotation at the tip of the forceps has begun from around 12 seconds.
Although small tracking errors can be seen, the reaction forces which acted on the slave device in *x*-*y* directions were reproducible to the master manipulator as tactile sense. In terms of above observations, it can be said that the effectiveness of the proposed control scheme was verified.

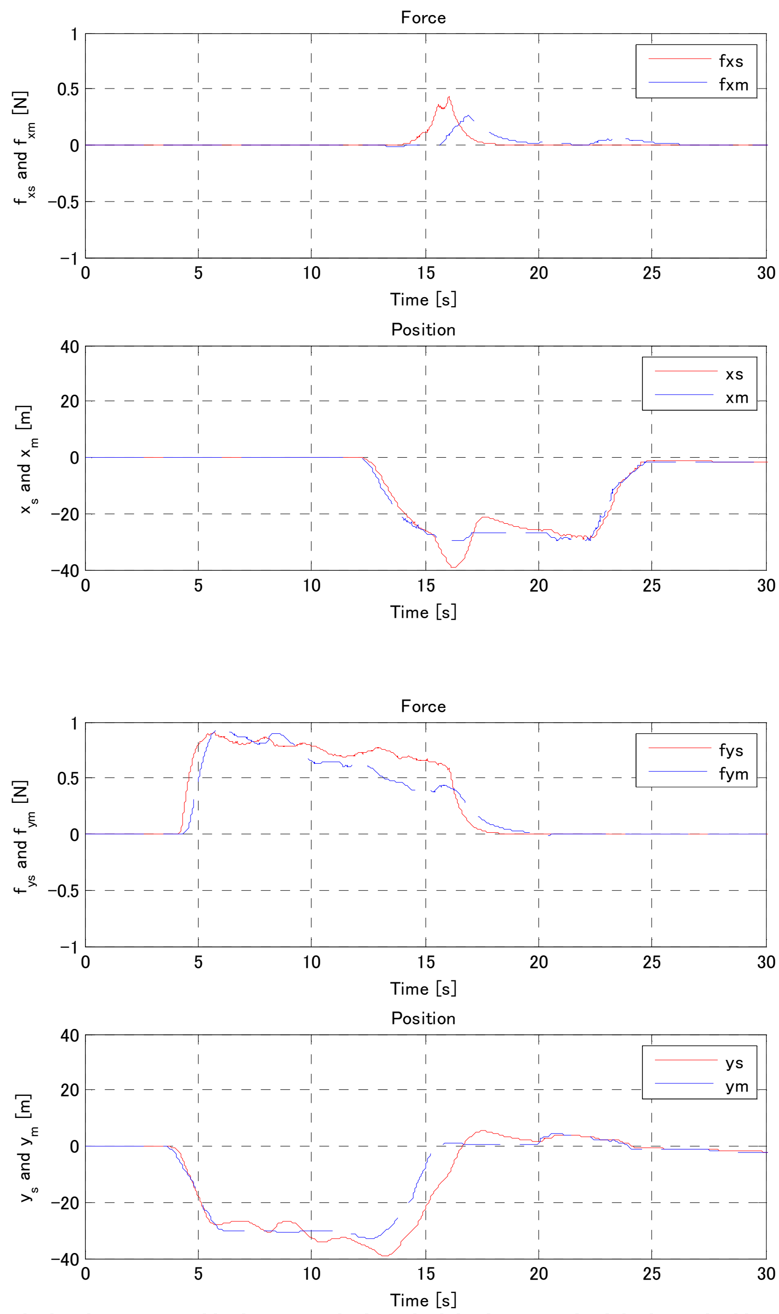

Fig. 19. Experimental results for omnidirectional bending of DSD robotic forceps

5. Conclusion

In this chapter, robust bilateral control for teleoperation systems in the presence of communication time delay was discussed. The Lyapunov function based bilateral control law that enables the motion scaling in both position tracking and force tracking, and guarantees stability of the system in the presence of the constant communication time delay, was proposed under the passivity assumption.
The proposed control law was applied to the haptic control of one-DOF bending motion of the DSD robotic forceps teleoperation system with constant time delay, and experimental works were executed.

In addition, the proposed bilateral control scheme was extended so that it may become applicable to the omnidirectional bending motion of the DSD robotic forceps. Experimental works for the haptic control of omnidirectional bending motion of the DSD robotic forceps teleoperation system with constant time delay were carried out. From the experimental results, the effectiveness of the proposed control scheme was verified.

6. Acknowledgement

The part of this work was supported by Grant-in-Aid for Scientific Research(C) (20500183). The author thanks H. Mikami for his assistance in experimental works.

7. References

Anderson, R. & Spong, M. W. (1989). Bilateral Control of Teleoperators with Time Delay, *IEEE Transactions on Automatic Control*, Vol.34, No. 5, pp.494-501

Arata, J., Mitsuishi, M., Warisawa, S. & Hashizume, M. (2005). Development of a Dexterous Minimally-Invasive Surgical System with Augumented Force Feedback Capability, *Proceedings of 2005 IEEE/RSJ International Conference on Intelligent Robots and Systems*, pp.3207-3212

Arata, J., Takahashi, H., Pitakwatchara, P., Warisawa, S., Tanoue, K., Konishi, K., Ieiri, S., Shimizu, S., Nakashima, N., Okamura, K., Fujino, Y., Ueda, Y., Chotiwan, P., Mitsuishi, M. & Hashizume, M. (2007). A Remote Surgery Experiment Between Japan and Thailand Over Internet Using a Low Latency CODEC System, *Proceedings of IEEE International Conference on Robotics and Automation*, pp.953-959

Chopra, N., Spong, M. W., Hirche, S. & Buss, M. (2003). Bilateral Teleoperation over the Internet: the Time Varying Delay Problem, *Proceedings of the American Control Conference*, pp.155-160

Chopra, N. & Spong, M.W. (2005). On Synchronization of Networked Passive Systems with Time Delays and Application to Bilateral Teleoperation, *Proceedings of SICE Annual Conference* 2005

Guthart, G. & Salisbury, J. (2000). The Intuitive Telesurgery System: Overview and Application, *Proceedings of 2000 IEEE International Conference on Robotics and Automation*, San Francisco, CA, pp.618-621

Ikuta, K., Yamamoto, K. & Sasaki, K. (2003). Development of Remote Microsurgery Robot and New Surgical Procedure for Deep and Narrow Space, *Proceedings of 2003 IEEE International Conference on Robotics & Automation,* Taipei, Taiwan, pp.1103-1108

Ishii, C.; Kobayashi, K.; Kamei, Y. & Nishitani, Y. (2010). Robotic Forceps Manipulator with a Novel Bending Mechanism, *IEEE/ASME Transactions on Mechatronics,* TMECH.2009.2031641, Vol.15, No.5, pp.671-684

Kobayashi, Y., Chiyoda, S., Watabe, K., Okada, M. & Nakamura, Y. (2002). Small Occupancy Robotic Mechanisms for Endoscopic Surgery, *Proceedings of International Conference on Medical Computing and Computer Assisted Intervention,* pp.75-82

Seibold, U., Kubler, B. & Hirzinger, G. (2005). Prototype of Instrument for Minimally Invasive Surgery with 6-Axis Force Sensing Capability, *Proceedings of 2005 IEEE International Conference on Robotics and Automation*, pp.496-501

Taylor, R. & Stoianovici, D. (2003). Medical Robotics in Computer-Integrated Surgery, *IEEE Transactions on Robotics and Automation*, Vol.19, No.5, pp.765-781

Yamashita, H., Iimura, A., Aoki, E., Suzuki, T., Nakazawa, T., Kobayashi, E., Hashizume, M., Sakuma, I. & Dohi, T. (2005). Development of Endoscopic Forceps Manipulator Using Multi-Slider Linkage Mechanisms, *Proceedings of 1st Asian Symposium on Computer Aided Surgery - Robotic and Image guided Surgery -*

Zemiti, N., Morel, G., Ortmaier, T. & Bonnet, N. (2007). Mechatronic Design of a New Robot for Force Control in Minimally Invasive Surgery, *IEEE/ASME Transactions on Mechatronics*, Vol.12, No.2, pp.143-153

Robust Control, Theory and Applications

Edited by Prof. Andrzej Bartoszewicz

ISBN 978-953-307-229-6
Hard cover, 678 pages
Publisher InTech
Published online 11, April, 2011
Published in print edition April, 2011

The main objective of this monograph is to present a broad range of well worked out, recent theoretical and application studies in the field of robust control system analysis and design. The contributions presented here include but are not limited to robust PID, H-infinity, sliding mode, fault tolerant, fuzzy and QFT based control systems. They advance the current progress in the field, and motivate and encourage new ideas and solutions in the robust control area.